FERMILAB-CONF-10-273-APC

W/Z + jet production at the Tevatron

Lars Sonnenschein[a]
on behalf of the DØ and CDF collaborations

[a] *RWTH Aachen University*
III. Phys. Inst. A
52056 Aachen, Germany.

Abstract

Vector boson plus jet production is interesting for Higgs search, beyond the Standard Model physics and provides standard candles for calibration. This is complementary to inclusive jet production measurements which provide precision tests of perturbative QCD. A multitude of W/Z plus heavy and light flavour jet measurements in $p\bar{p}$ collisions at a centre of mass energy of $\sqrt{s} = 1.96$ TeV is discussed. Next-to-Leading order perturbative QCD predictions and various models are compared to the measurements.

1. Introduction

The discussed measurements are accomplished by the multi-purpose collider experiments DØ and CDF with their broad particle identification capabilities through central tracking, fine granulated calorimeters and muon spectrometers. The detectors are located at the Tevatron accelerator at Fermilab, where proton anti-proton collisions take place at a centre of mass energy of 1.96 TeV. Vector boson plus jet production at the Tevatron is complementary to the kinematic regimes of the HERA accelerator and fixed target experiments. It provides handles to Parton Distribution Functions (PDF), initial and final state gluon radiation and the transverse momentum (p_T) spectra of the jets and the vector bosons. The measurements provide standard candles for calibration and tuning of Monte-Carlo (MC) event generators. The understanding of these processes is important for Standard Model (SM) as well as Beyond the SM (BSM) phenomenology. The Tevatron dataset is now large enough to confront predictions and it has a unique kinematic overlap with the LHC and the expected SM Higgs mass range.

The data of the measurements are fully corrected for instrumental effects. Therefore they can be directly used for testing and improving existing MC event generators and any future calculation and model. Next-to-Leading Order (NLO) and Leading Order (LO) perturbative QCD (pQCD) predictions from MCFM [1] are compared to data taking non-perturbative effects of hadronisation and underlying event from simulation into account in the prediction, i.e. the comparison takes place at the hadronic final state or synonymous at the particle level. The relative uncertainties of the measurements are dominated by the Jet Energy Scale (JES) uncertainty. Iterative seed-based infrared safe midpoint cone jet algorithms are used by the DØ [2] and CDF [3] experiments in Run II.

In the following sections 2-6 the Tevatron vector boson plus light flavour jet measurements are presented, followed by the vector boson plus heavy flavour jet measurements in sections 7-11.

2. DØ inclusive $Z/\gamma^*(\rightarrow ee)$ + jet cross section

The Z + jet production cross section is measured [4] differentially in inclusive p_T bins of leading, second and third leading jet, making use of an integrated luminosity of 1.0 fb^{-1}. Electron/positron candidates above a transverse momentum of $p_T > 25$ GeV are selected in an absolute pseudorapidity range of $|\eta_e| < 1.1, 1.5 < |\eta_e| < 2.5$ to form Z boson candidates in a mass window of $65 < M_{ee} < 115$ GeV. Jets with a cone radius of $R = 0.5$ and a $p_T^{\rm jet} > 20$ GeV are selected in a rapidity range of $|y_{\rm jet}| < 2.5$. The cross section is normalised to inclusive Z + jet production which cancels uncertainties on luminosity and most of electron trigger and identification uncertainties. The phase space of the selected events is extrapolated to the full lepton kinematics. While the (N)LO pQCD predictions are in agreement with data there are large differences between the different models of PYTHIA [5], HERWIG [6] (+ JIMMY), ALP-

GEN [7] + PYTHIA and SHERPA [8]. The experimental errors are small and dominated by statistics, allowing for future improvements.

3. CDF inclusive $Z/\gamma^*(\rightarrow ee)$ + jet cross section

The Z + jet production cross section is measured [9] differentially in inclusive transverse momentum bins of the leading and second leading jet, making use of an integrated luminosity of 1.7 fb^{-1}. Electron/positron candidates above a transverse energy of $E_T^e > 25$ GeV are selected in an absolute pseudorapidity range of $|\eta_e| < 1.0, 1.2 < |\eta_e| < 2.8$ to form Z boson candidates in a mass window of $66 < M_{ee} < 116$ GeV. Jets with a cone radius of $R = 0.7$ and a $p_T^{\rm jet} > 30$ GeV are selected in a rapidity range of $|y_{\rm jet}| < 2.1$. There is good agreement between data and NLO pQCD prediction.

4. DØ inclusive $Z/\gamma^*(\rightarrow \mu\mu)$ + jet cross section

Differential angular distributions of the Z + jet production cross section is measured [10] in inclusive bins of transverse Z boson momentum making use of an integrated luminosity of 1.0 fb^{-1}. Oppositely charged muon candidates above a threshold of $p_T > 15$ GeV are selected in an absolute rapidity range of $|y_\mu| < 1.7$ to form Z boson candidates in a mass window of $65 < M_{\mu\mu} < 115$ GeV. Jets with a cone radius of $R = 0.5$ and a $p_T^{\rm jet} > 20$ GeV are selected in a rapidity range of $|y_{\rm jet}| < 2.8$. The differential cross section in two inclusive bins of Z boson transverse momentum ($p_T^Z > 25$ GeV and $p_T^Z > 45$ GeV) is measured as a function of the angular variables rapidity sum, rapidity difference and the azimuthal angle difference between the leading jet and the Z boson. ALPGEN [7] and SHERPA [8] include up to three partons in the matrix element calculations. The binning is chosen such, that the detector resolution causes little migrations between bins. There is less agreement between data and predictions in the lower $p_T^Z > 25$ bin. This holds for the non-pQCD as well as for the pQCD predictions. Among the non-pQCD predictions SHERPA (1.1.3) provides the best description of the angular distributions, in particular $\Delta y(Z, j)$, in the $p_T^Z > 45$ GeV bin. In the $p_T^Z > 25$ GeV bin the measured cross section is $\sigma(Z + \text{jet})/\sigma(Z) = [47 \pm 1(\text{stat.}) \pm 2(\text{syst.})] \cdot 10^{-3}$ compared to the pQCD NLO prediction of $[40 \pm 3(\text{scale}) \pm 1(\text{PDF})] \cdot 10^{-3}$ and the pQCD LO prediction of $[40 \pm 8(\text{scale}) \pm 1(\text{PDF})] \cdot 10^{-3}$.

5. CDF $Z(\rightarrow ee, \mu\mu)$ + 1 jet p_T balance

CDF measured the Z boson + 1 jet exclusive p_T balance [11], making use of an integrated luminosity of 4.6 fb^{-1} and sets precision limits on the measurements of Standard Model (SM) jet and vector boson observables, relevant for the discovery potential of new physics. Oppositely charged lepton candidates ($\ell = e, \mu$) above a threshold of $p_T^\mu, E_T^e > 18$ GeV are selected to form Z boson candidates in a mass window of $80 < M_{\mu\mu} < 100$ GeV. A leading jet with a $p_T^{\rm jet} > 8$ GeV is selected in a pseudorapidity range of $0.2 < |\eta_{\rm jet}^{\rm det}| < 0.8$ to avoid cracks in the central calorimeter. The measurement is accomplished for three different cone algorithm radii $R = 0.4, 0.7, 1.0$. The azimuthal angle between the Z boson and the jet has to satisfy $\Delta\phi > 3.0$ rad to provide back-to-back configurations in the plane transverse to the beam axis. Predictions for Z boson + jet production are obtained from PYTHIA [5] and ALPGEN [7]. The CDF JES is calibrated via tuning of the calorimeter response to single particles. Therefore the Z boson plus jet p_T balance provides an independent test of the CDF JES. While the measured track in jet distributions agree

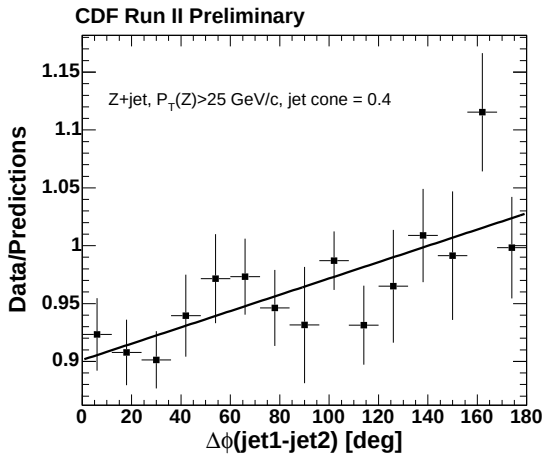

Figure 1: Leading jet plus Z boson p_T balance data over simulation (PYTHIA) ratio as a function of the azimuthal angle difference between the leading and the second leading jet. Data has more sub-leading jets close in angle to the leading jet.

with the quark and gluon jet fractions of PYTHIA [5], a higher rate of sub-leading jets collinear to the leading jet is observed in data (see Fig. 1). This does set limitations on the precision of the JES determined at the ATLAS and CMS experiments by means of the jet plus Z boson p_T balance of the order of 3%. Only large angle final state radiation observed in form of sub-leading jets turns out to be able to explain the discrepancy.

6. CDF inclusive $W(\rightarrow e\nu)$ + n=1-4 jets cross section

The $W + n$ jet inclusive production cross section ($n = 1 - 4$) is measured [12] differentially in inclusive transverse momentum bins of the nth leading jet, making use of an integrated luminosity of $320\,\mathrm{pb}^{-1}$. Electron/positron candidates above a transverse energy of $E_T^e > 20\,\mathrm{GeV}$ are selected in an absolute pseudorapidity range of $|\eta_e| < 1.1$. A missing transverse energy of $\not{E}_T > 30\,\mathrm{GeV}$ and a transverse mass of $m_T^W > 20\,\mathrm{GeV}$ is required to select W boson candidates. Jets with a cone radius of $R = 0.4$ and a $p_T^{\mathrm{jet}} > 20\,\mathrm{GeV}$ are selected in a pseudorapidity range of $|\eta_{\mathrm{jet}}| < 2.0$. The measurement benefits of a production cross section which is about ten times higher than the one for Z + jets production. At the same time the multi-jet and top quark production background needs to be controlled. There is good agreement between data and the NLO pQCD prediction. At low transverse jet momentum the MC event generators ALPGEN [7] plus PYTHIA [5] (with MLM matching of the matrix element to the parton shower) and MADGRAPH [13] plus HERWIG [6] (with CKKW matching) need a better modelling of the underlying event.

7. DØ inclusive $\sigma(Z+b)/\sigma(Z+j)$ ratio ($Z \rightarrow ee, \mu\mu$)

The inclusive $Z + b$ jet production cross section is measured [14] as the ratio over the inclusive Z + jet production cross section, making use of an integrated luminosity of $4.2\,\mathrm{fb}^{-1}$. Z boson decays into a pair of charge conjugated electrons or muons are considered. Muon candidates with $p_T^{\mu} > 10\,\mathrm{GeV}$ in the pseudorapidity range of $|\eta_{\mathrm{det}}| < 2.5$ and electron/positron candidates with $p_T^e > 15\,\mathrm{GeV}$ in the pseudorapidity range of $|\eta_{\mathrm{det}}| < 2.0$ are selected together with jets ($R = 0.5$). The leading jet has to have a transverse momentum of $p_T^{\mathrm{jet}} > 20\,\mathrm{GeV}$ in a pseudorapidity range of $|\eta_{\mathrm{det}}| < 1.1$. The b flavour jets are separated from c and light flavour jets by means of a neural network jet tagging algorithm based on the longer mean lifetime of heavy flavour hadrons with respect to light ones. The flavour fractions are determined by a fit of lifetime variable templates to the data. The templates are obtained from ALPGEN [7] plus PYTHIA [5] while the cross sections are taken from NLO pQCD calculations. The measured total cross section ratio is $\sigma(Z+b)/\sigma(Z+j) = 0.0176 \pm 0.0024(\mathrm{stat.}) \pm 0.0023(\mathrm{syst.})$ consistent with the NLO pQCD prediction of 0.0184 ± 0.0022.

8. CDF inclusive $\sigma(Z + b)/\sigma(Z)$ ratio ($Z \rightarrow ee, \mu\mu$)

The inclusive $Z + b$ jet production cross section is measured [15] as the ratio over the inclusive Z production cross section, making use of an integrated luminosity of $2.0\,\mathrm{fb}^{-1}$. Z boson decays into a pair of charge conjugated electrons or muons are considered. The cross section is measured differentially in bins of jet and heavy flavour jet multiplicity, as functions of leading b jet transverse energy and pseudorapidity and as a function of the Z boson transverse momentum. b jets are identified by means of a secondary vertex tagging algorithm. The leading and second leading leptons (e, μ) are required to satisfy $p_T^{\mu_1}, E_T^{e_1} > 18\,\mathrm{GeV}$ and $p_T^{\mu_2}, E_T^{e_2} > 10\,\mathrm{GeV}$. The invariant dilepton mass has to lie in the interval $76 < M_{\ell\ell} < 106\,\mathrm{GeV}$. Jets with a cone radius of $R = 0.7$ and a $E_T^{\mathrm{jet}} > 20\,\mathrm{GeV}$ are selected in a pseudorapidity range of $|\eta_{\mathrm{jet}}| < 1.5$. The measured cross section ratio $\sigma(Z{+}b)/\sigma(Z) = [3.32 \pm 0.53(\mathrm{stat.}) \pm 0.42(\mathrm{syst.})] \times 10^{-3}$ is in agreement with NLO pQCD predictions. Both data and theory have large uncertainties. While data uncertainties are statistics dominated the large uncertainty of the theory prediction arises from the missing NLO pQCD prediction for $Z + b\bar{b}$ production which in turn causes a large scale dependence.

9. DØ inclusive $\sigma(W + c)/\sigma(W + j)$ ratio ($W \rightarrow \ell\nu$)

The inclusive $W + c$ jet production cross section is measured [16] as the ratio over the inclusive W + jet production cross section, making use of an integrated luminosity of $1.0\,\mathrm{fb}^{-1}$. The leptonic W boson decay with a muon/electron in the final state is considered. The cross section is measured differentially in bins of jet p_T. Lepton candidates with $p_T^{\ell} > 20\,\mathrm{GeV}$ and events with a missing transverse energy of $\not{E}_T > 20\,\mathrm{GeV}$ are selected. Jets with a cone radius of $R = 0.5$ and $p_T^{\mathrm{jet}} > 20\,\mathrm{GeV}$ are selected in a pseudorapidity range of $|\eta_{\mathrm{jet}}| < 2.5$. W boson + c quark production is sensitive to the s quark PDF content up to scales of $Q^2 = 10^4\,\mathrm{GeV}^2$. The charge sign of the lepton from the W boson decay is opposite (OS) to the one of the c quark. This information is exploited in tagging an oppositely charged muon in the jet from the c quark fragmentation. The same sign (SS) subtracted background is small ($\sim 1\%$). The multi-jet background is determined from data. The measured cross section is corrected for acceptances and efficiencies. It amounts to $\sigma(p\bar{p} \rightarrow W + c{-}\mathrm{jet})/\sigma(p\bar{p} \rightarrow W + \mathrm{jets}) = 0.074 \pm 0.019(\mathrm{stat.})^{+0.012}_{-0.014}(\mathrm{syst.})$ and is within the large errors in agreement with the prediction of 0.044 ± 0.003 from ALPGEN [7] plus PYTHIA [5].

10. CDF semi-incl. $W + c$ jet cross section ($W \to \ell\nu$)

The $W + c$ jet exclusive production cross section is measured [17] for selected events with one or two jets, making use of an integrated luminosity of $1.8\,\mathrm{fb}^{-1}$. Lepton candidates with $p_T^{\ell} > 20\,\mathrm{GeV}$ in the pseudorapidity range of $|\eta_\ell| < 1.1$ and events with a missing transverse energy of $\not\!\!E_T > 25\,\mathrm{GeV}$ are selected. Jets with a cone radius of $R = 0.4$ and $p_T^{\mathrm{jet}} > 20\,\mathrm{GeV}$ are selected in a pseudorapidity range of $|\eta_{\mathrm{jet}}| < 1.5$. Charm flavour jets are tagged by means of a soft muon in the jet. The OS-SS subtracted data distributions are in good agreement with the prediction of ALPGEN [7] with PYTHIA [5]. The total measured cross section amounts to $\sigma(W_{(\to\ell\nu)}+c) = 9.8\pm2.8(\mathrm{stat.})^{+1.4}_{-1.6}(\mathrm{syst.})\pm0.6(\mathrm{lum.})$ pb and is in good agreement with the NLO pQCD prediction of $\sigma(W_{(\to\ell\nu)} + c) = 11.0^{+1.4}_{-3.0}$ pb for $p_T^{c\text{-jet}} > 20$ GeV and $|\eta_{c\text{-jet}}| < 1.5$.

11. CDF semi-incl. $W + b$ jet cross section ($W \to \ell\nu$)

The $W + b$ jet exclusive production cross section is measured [18] for selected events with one or two jets, making use of an integrated luminosity of $1.9\,\mathrm{fb}^{-1}$. The leptonic W boson decay with a muon/electron in the final state is considered. Lepton candidates with $p_T^{\ell} > 20\,\mathrm{GeV}$ and $|\eta_\ell| < 1.1$ and events with a missing transverse energy of $\not\!\!E_T > 25\,\mathrm{GeV}$ are selected. Jets with a cone radius of $R = 0.4$ and $p_T^{\mathrm{jet}} > 20\,\mathrm{GeV}$ are selected in a pseudorapidity range of $|\eta_{\mathrm{jet}}| < 2.0$. Bottom flavour jets are tagged by means of a secondary vertex tagging algorithm. A maximum likelihood fit to the vertex mass distribution of tagged jets is applied to extract the flavour fractions of the selected data sample. The flavour templates are obtained from ALPGEN [7] with PYTHIA [5] and MADEVENT [19] for single top quark production. The measured total cross section is $\sigma(W_{(\to\ell\nu)} + b) = 2.74 \pm 0.27(\mathrm{stat.}) \pm 0.42(\mathrm{syst.})$ pb. This has to be compared to the NLO pQCD prediction of $\sigma(W_{(\to\ell\nu)} + b) = 1.22 \pm 0.14$ pb and the LO prediction of $\sigma(W_{(\to\ell\nu)} + b) = 0.78$ pb from ALPGEN. The measured cross section exceeds the NLO prediction by about three σ standard deviation.

12. Conclusions

Many measurements of vector boson plus light and heavy flavour jet production have been presented. Perturbative QCD predictions by means of MCFM [1] are in good agreement with data in all inclusive vector boson plus jet production measurements. The predictions of ALPGEN and MCFM are about three σ below the exclusive W boson plus b jet cross section measurement of CDF, where a reliable secondary vertex tagger has been used. The jet over Z boson p_T balance measurement of CDF shows up limitations for the Jet Energy Scale precision at LHC experiments of the order of 3%. The p_T imbalance can be explained by large angle final state radiation in form of collinear sub-leading jets. There is no perfect Monte-Carlo event generator. This holds for PYTHIA and HERWIG+JIMMY as well as for SHERPA and ALPGEN which are superior to the former parton shower Monte-Carlo event generators. In general the data are corrected for detector effects, so that they can be compared to predictions at the hadronic final state. This means that the data can be re-used for the tuning of Monte-Carlo event generators at any time in the future.

Acknowledgements

Many thanks to the staff members at Fermilab, collaborating institutions and in particular the DØ and CDF collaborations.

References

[1] J. Campbell and R. K. Ellis, Phys. Rev. D **65**, 113007 (2002).
[2] G. C. Blazey *et al.*, in *Workshop Proceedings: QCD and Weak Boson Physics in Run II*, ed. by U. Bauer, R. K. Ellis and D. Zeppenfeld, FERMILAB-PUB-00-297 (2000).
[3] A. Abulencia *et al.* (CDF collaboration), Phys. Rev. D **74**, 071103(R) (2006), A. Bhatti *et al.*, Nucl. Instrum. Meth. A. **566**, 375 (2006).
[4] V. M. Abazov *et al.* (DØ collaboration), arXiv:0903.1748v2, FERMILAB-PUB-09-066-E, Phys. Lett. B **678**, 45 (2009).
[5] T. Sjöstrand *et al.*, JHEP **0605**, 026 (2006).
[6] G. Corcella *et al.*, JHEP **0101**, 010 (2001).
[7] M. L. Mangano *et al.*, JHEP **0307**, 001 (2003).
[8] T. Gleisberg *et al.*, JHEP **0902**, 007 (2009).
[9] T. Altonen *et al.* (CDF collaboration), Phys. Rev. Lett. **100**, 102001 (2008).
[10] V. M. Abazov *et al.* (DØ collaboration), arXiv:0907.4286v2, FERMILAB-PUB-09-373-E, Phys. Lett. B **682**, 370 (2010).
[11] T. Altonen *et al.* (CDF collaboration), prel., CDF note 10082, submitted to Nucl. Instrum. Meth. A (2010).
[12] T. Altonen *et al.* (CDF collaboration), Phys. Rev. D **77**, 011108(R) (2008).
[13] F. Maltoni and T. Stelzer, J. High Energy Phys. 02 (2003) 027.
[14] V. M. Abazov *et al.* (DØ collaboration), prel., DØ note 6053-CONF (2010).
[15] T. Altonen *et al.* (CDF collaboration), Phys. Rev. D **79**, 052008 (2009).
[16] V. M. Abazov *et al.* (DØ collaboration), arXiv:0803.2259v1, FERMILAB-PUB-08-062-E, Phys. Lett. B **666**, 23 (2008).
[17] T. Altonen *et al.* (CDF collaboration), Phys. Rev. Lett. **100**, 091803 (2008).
[18] T. Altonen *et al.* (CDF collaboration), Phys. Rev. Lett. **104**, 131801 (2010).
[19] J. Alwall *et al.*, Journ. HEP **0709**, 028 (2007).